TiO_2 supported natural zeolites as biogas enhancers through photocatalytic pre-treatment of *Miscanthus x giganteous* crops.

S. TEDESCO [*a,b], G. HURST [a], A. IMTIAZ [a], M. RATOVA [b], L. TOSHEVA [c], P. KELLY [b]

[*a] Department of Mechanical Engineering, School of Mechanical Engineering, Manchester Metropolitan University, Dalton Building, Chester Street, Manchester, M1 5GD.

[b] Advanced Materials and Surface Engineering (AMSE) Research Centre, Manchester Metropolitan University, Dalton Building, Chester Street, Manchester, M1 5GD.

[c] School of Science and Environment, Manchester Metropolitan University, Manchester, M1 5GD.

Declarations of interest: none.

Abstract

Miscanthus giganteous is probably the most fast growing and low nutrient bioenergy crop among lignocellulosic feedstocks. Despite its significant content in fermentable sugars, currently *Miscanthus* biomass is not used for biogas/methane production due to the high-lignin and low moisture content in the winter/spring harvest as well as cellulose crystallinity, which limit access to enzymatic action for all lignocellulosic feedstock. This study identified that a photocatalytic pretreatment prior to anaerobic digestion helps increase the substrate's biodegradability by oxidising the lignin fraction, leading to increased methane yield up to 46% compared to the untreated. A novel photocatalyst was manufactured by reactive magnetron-sputtering deposition of TiO_2 particles onto natural zeolite supports, which provided important trace elements for the anaerobic digestion process and retained a large surface area that acted as biofilm to boost growth of the microbial community. A load of 2% w/w catalyst in the bioreactor after 3 hours of photocatalytic treatment led to 220 mL_N gVS^{-1}, with a net energy balance that is achieved for the whole process when treating the dispersed phase suspension at concentrations above 10 g m^{-3}.

Keywords: Biogas; Anaerobic digestion; Lignocellulosic; Photocatalysis; Pretreatment; Zeolites.

* Corresponding author: Department of Mechanical Engineering, School of Mechanical Engineering, Manchester Metropolitan University, Dalton Building, Chester Street, Manchester, M1 5GD. E-mail address: silvia.tedesco3@mail.dcu.ie, s.tedesco@mmu.ac.uk. Tel.: +44 161 247 6259

1. Introduction:

Lignocellulosic biomass, known as second-generation feedstock for biofuels, is readily found in nature and consists of non-edible crops and their residues from the forestry and agricultural industry. Lignocellulosic crops are regarded as carbon neutral (and therefore are not involved in the *food versus fuel* debate) to produce bioenergy as the carbon dioxide captured from the environment by the plant in its life cycle is then released during combustion of biofuels. Anaerobic digestion (AD) is regarded as the most established route to bioenergy, resulting in a renewable gaseous energy carrier (biogas) and a digestate by-product (fertiliser). Biogas can be used to supply heat and electricity (CHP) or as gaseous fuel (biomethane) for grid injection or as transport fuel. Lignocelluloses are mainly made of cellulose and hemicellulose (C5-C6 fermentable sugars), bound together by lignin, an aromatic polymer refractory to energy conversion. Lignin's strong (covalent and dipolar) bonds to cellulose and hemicellulose are the main bottleneck for conversion of terrestrial plants [1] to biogas. Degradation by cellulosic enzymes is limited by % of lignin in the substrate, as it prevents access to fermentable carbohydrates. Hence, the Biochemical Methane Potential (BMP) decreases as lignin content increases [2, 3].

Among the different types of purposely grown energy crops, *Miscanthus x giganteous* is a cheap, non-edible, fast growing perennial crop exhibiting high carbohydrates content (>60% [4, 5]) with biogas yields comparable to maize crops [6], which is often the most grown land crop for biomethane generation via AD. Cultivation of *Miscanthus x giganteous* is particularly advantageous, due to its extremely low water and nutrient requirements, along with fast growing rates of 9–18 t ha^{-1}[6] dry matter. *Miscanthus* species are not currently used for biogas production based on the high lignin and low moisture content in the winter/spring harvest. Also, fermentable carbohydrates are trapped by the crystalline structure of cellulose as well as the lignin (acid insoluble 20-30% [4, 5]). To increase the BMP, typically one or more custom, and often expensive, pretreatments are employed with the scope of breaking down the cellulose crystallinity, degrading lignin, hydrolysing complex carbohydrates and increasing the surface area available to enzymatic action.

Very recently, heterogeneous photocatalysis has been identified as a possible sustainable approach to lignin valorisation [7] of lignocellulosic feedstocks, particularly when using nanomaterial catalysts, due to their selective transformations of biomass-derived compounds. This approach offers great environmental benefits, including low energy consumption as well

as the opportunity for catalyst recovery and regeneration. Among semiconducting oxides for photocatalysis applications, TiO_2 in anatase has been determined to be the most efficient in relation to its high selectivity towards carboxylic acids [8], stability, high photocatalytic efficiency, low toxicity and low cost. High optical absorbance in the near-UV region remains the major advantage of TiO_2 for photocatalytic pre-treatments. Lignin photo-oxidation through exposure to UV radiation has been reported [8] to produce aromatic aldehydes and carboxylic acids, and overall enhance the solubility of refractory compounds. A very recent scientific study [9] has utilised photocatalytic pretreatments with TiO_2 (1.5% w/w) to break down the lignin component of wheat straw and measured the main products of such oxidation in vanillic and ferulic acids. Such products were found not to inhibit biogas production and the effectiveness of the pretreatment showed improved yields at highest oxidation times (2-3 hours) of up to 37% in BMP tests and 25% in CSRT.

Furthermore, due to imbalance of the C:N ratio when fermenting lignocelluloses to methane (>>30), the development of microbial inhibitors is likely to occur during the formation of hydrolysates when high organic loadings are fed to the microorganisms, unless the substrate is co-digested with appropriate feedstock. In order to decrease the impact of developing inhibiting phenomena, inexpensive inorganic additives, such as zeolites, can be supplied to the digester with the result of a boosted methane production. Clinoptilolite is a natural zeolite found in most mine deposits worldwide. Thanks to its microporous arrangement of silica and alumina tetrahedral structures, it has excellent cation exchange properties, a good surface area (CLT-R has an S_{BET} of about 20-30 m^2/g [10]) and has high affinity for NH_4^+ binding with the result of reducing the lag phase in AD. Zeolites are often used in AD to boost growth of microbial population and buffer the rates of enzymatic transformation of compounds [11] such as ammonium, sulphur, carbohydrates and protein-rich materials. This study investigates the effect of a composite photocatalyst that combines the benefits of photocatalytic depolymerisation of lignin at mild conditions with that of prevention/mitigation of inhibition using inorganic additives. For this purpose, TiO_2 granules have been annealed onto zeolite (clinoptilolite) supports using a magnetron-sputtering rig and, subsequently, used in a photocatalytic treatment prior to anaerobic fermentation. Methane yields are compared with those from other lignocellulosic feedstocks that have undergone pre-treatments, finally a net energy balance is derived to draw conclusions on the economic viability of the process. The visual changes in biomass structure were studied by SEM, XRD, FTIR, while surface appraisal of the engineered composite photocatalyst were analysed via SEM, EDX, XRD and BET.

2. Materials and Methods:

2.1. Compositional and analytical methods

Miscanthus x giganteous biomass was provided by a local grower in the UK, ground to <0.2 mm using a ball mill, then stored in a desiccator until use. The inoculum sludge consisted of brewery and distillery effluents collected from full-scale digesters at an industrial organic waste treatment plant located in Greater Manchester, United Kingdom. Total Solids (TS) and Volatile Solids (VS) of the samples were characterised using a high-temperature oven via overnight drying at 105 °C followed by combustion at 575°C, as by standard procedure [12]. All tests were conducted in triplicate.

The ultimate analysis of *Miscanthus* was outsourced to a biomass laboratory (Celignis Ltd.) to identify the elemental composition of the samples after drying. The carbon, hydrogen, nitrogen, and sulphur contents of biomass samples were obtained according to the European Standard procedure EN 15104:2011 [13], using an Elementar Vario MACRO Cube elemental analyser, while the inoculum characterisation was performed with a carbolite furnace according to [14]. The oxygen content was calculated by difference according to the formula below:

Oxygen (%) = 100 - Carbon(% Dry Basis) - Hydrogen(% Dry Basis) - Nitrogen(% Dry Basis) -Sulphur(% Dry Basis) - Ash(% Dry Basis) eq. (1)

After filtering the solids (0.2 μm), High performance Liquid Chromatography (HPLC) was used to measure water soluble sugars using a modified NREL protocol [15], with an HP-1100 HPLC with an Agilent 1200 Refractive Index Detector (RID) equipped with a Bio-Rad Aminex HPX-87H column (Bio-Rad Laboratories). The temperature was maintained at 55 ˚C and 5 mM H_2SO_4 was used as the mobile phase with the flowrate maintained at 0.6 ml/min [15].

The functional group change of the untreated and post treatment *Miscanthus* was analysed by Fouruier Transform Infrared (FTIR) using a Spectrum Two spectrophotometer (Perkin Elmer). Cellulose, hemicellulose and lignin (Klason) contents were determined according to NREL/TP-510-42618. The crystallinity index (CI) of the substrate before and after treatment was determined by X-ray diffraction (XRD) using a PANalytical X'Pert Powder system (Pananalytical), operated at 40mA and 45kV. The biomass CI in % was calculated as per eq. (2) by Segal et al. [16]:

$$CI(\%) = \left[\frac{I_{002} - I_{am}}{I_{002}}\right] x\ 100$$

eq. (2)

where I_{002} is the intensity of the diffraction at 002 peak position ($2\theta \approx 22.5°$) for cellulose and I_{am} is the peak for the amorphous region at about $2\theta \approx 17.9°$.

2.2. Photocatalyst deposition and analysis

Magnetron-sputtering annealing was selected for depositing TiO_2 for a trifold benefit: the technique allows for thin layer deposition (avoiding clog of cavities, a compromise to retain the highest surface area was sought in this study), low energy consumption and no use of solvents, meaning it is cheap as well as sustainable when compared to most coating techniques. Also after use, the zeolite supports (0.7-1.6 mm) can easily be sieved out of the photolysed suspension and undergo different regeneration methods using electrochemical, stripping, drying and other common recovery techniques.

TiO_2 coatings were deposited in a vacuum coating system utilising two planar unbalanced type II magnetrons (Teer Coatings Ltd., Droitwich, UK),) installed in a closed field configuration in the top of the vacuum chamber facing the substrate holder schematic representation of the deposition setup is given in the Figure 1(A). Solid titanium targets (300 mm × 100 mm, 99.5% purity) were fitted to both magnetrons. The sputtering process was carried out in the reactive mode in argon/oxygen atmosphere at partial pressure of 0.4 Pa for a total time of 90 min. The flow of both gases was controlled with mass-flow controllers; the flow of Ar was 15 sccm, flow of oxygen 20 sccm. The magnetrons were powered in pulsed DC (pDC) mode with dual channel Advanced Energy Pinnacle Plus power supply at pulse frequency of 100 kHz and duty of 50%.

Deposition of titanium dioxide coatings onto loose zeolite substrates was enabled via use of the oscillator bowl (the detailed description of the oscillating mechanism is given elsewhere [17, 18]. For deposition run, a 50g charge of zeolite support (R&D Laboratories Ltd.) was loaded into the bowl. As titanium dioxide coatings tend to be amorphous in as-deposited form, the samples were post-deposition annealed in air at 673K and then allowed to cool gradually (5–6 h) to avoid the formation of the thermal stresses in the coatings (the annealing temperature has been pre-defined experimentally to ensure crystallinity development for titanium dioxide [19].

The compositional analysis of the coated zeolites was conducted through an energy-dispersive X-ray spectroscopy (EDX), utilising a AMETEK EDAX TSL. The TiO_2 particles dispersion

onto the zeolites support and the surface images were obtained with scanning electron microscopy (SEM) (Zeiss Supra 40 VP-FEG-SEM, Germany). The specific surface areas of the samples were determined with Brunauer–Emmett–Teller (BET) surface area measurements, using a Micromeritics ASAP2020 system. Samples were heated for 12 h at 300◦C prior to analysis and surface areas were calculated from nitrogen adsorption data in the range of relative pressures between 0 and 1 using the BET model. Total pore volumes were determined from the measurements at p/p_0 of 0.99 using a density conversion factor of 0.001547. External surface areas and micropore areas were determined by the t-lot method.

Finally, SEM was also used to visually evaluate the structural differences between untreated and pretreated *Miscanthus* biomass induced by UV irradiation.

2.3. Photocatalytic pretreatment

To carry out the photocatalytic treatment, a low-pressure UV mercury bench lamp (2×Sankyo Denki BLB lamps, peaked at 352 nm was used (irradiance patterns are given by Figure 2 and fully described elsewhere [19]). The *Miscanthus x giganteous* biomass (5% w./w., i.e. 2.5 g) was diluted with deionised water (50 mL) as medium for the dispersed phase in beakers of 150 ml capacity. The solution was homogeneously mixed with magnetic stirrers (fixed at 200 RPM) throughout the treatment duration, see Figure 1(B), to maximised the exposure of the whole mixture.

The photocatalytic treatment with the coated photocatalyst was conducted for 3 hours after a dark period of 30 mins as per Orti-Gomez et al. [20], during which the reactants were left in contact with the catalyst before the UV lamp was turned on.

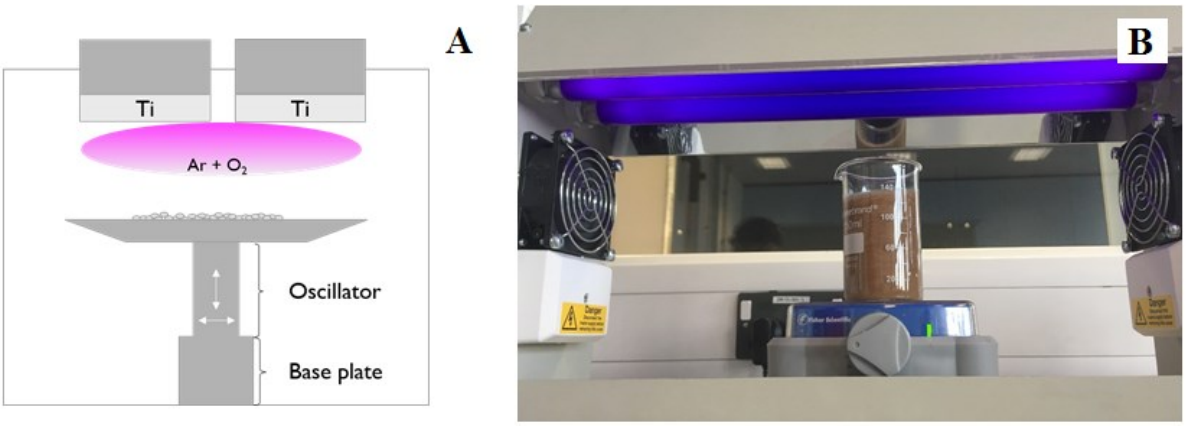

Figure 1 Schematic representation of the sputtering rig used for deposition of titanium dioxide (A) and photocatalytic treatment system (B)

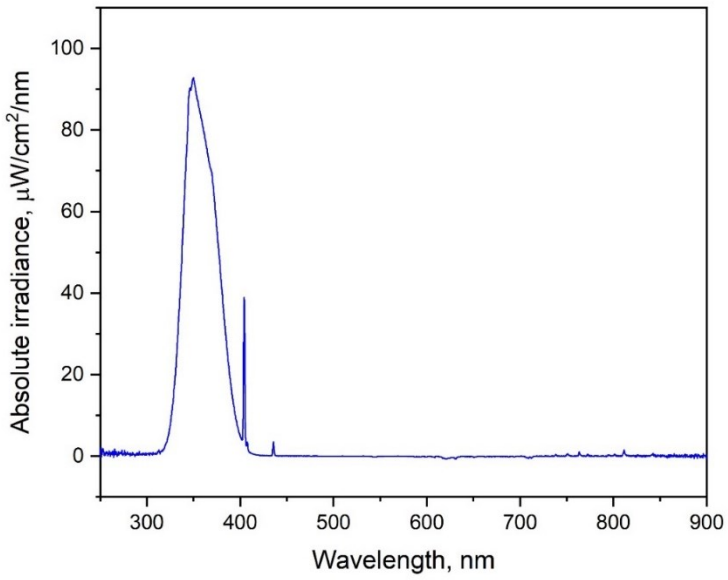

Figure 2 Irradiance patterns of the UV equipment used

2.4. Biomethane potential assays

In addition to the fermentation of inoculum alone, AD of inoculum with added zeolites was also tested to estimate the effect of the zeolite supports for biogas production. The biochemical methane potential (BMP) was conducted following the VDI 4630 procedure [21] for anaerobic fermentation of organic materials. The reactors consisted of borosilicate glass flasks of 500 ml each in capacity, which used an inoculum-to-substrate ratio of 4:1 on a wet weight basis.

A biogas analyser, model GeoTech GA5000plus, was used to verify anaerobic conditions were created correctly when preparing the reactors and to analyse the gas composition at the end of the collection period. An upturned measuring cylinder was utilized to derive the dry biogas

volume by water displacement and the methane yields are reported for a gas in standard conditions (0 °C, 1 atm). The system was cleared up from oxygen/air traces via nitrogen flushing prior to seeding for BMP. Water-baths were used to keep the reactors at a fixed mesophilic temperature of 29 ± 1 °C with a short retention time of 15 days. A control sample of inoculum in double replication was used to determine its contribution to the biogas formation, which was then subtracted from the total biogas digestion volume in order to determine the actual yields of *Miscanthus x giganteous*.

2.5 Stoichiometric yields and anaerobic biodegradability

The stoichiometric methane potential (SMP) was derived from the elemental analysis described in section 2.1, using Buswell equation [22] (eq. (3)). The obtained SMP yields identify the maximum theoretical methane that can be achieved from the substrate.

$$C_cH_hO_oN_nS_s + 1/4(4c - h - 2o + 3n + 2s)H_2O = 1/8(4c + h - 2o - 3n - 2s)CH_4 + 1/8(4c - h + 2o + 3n + 2s)CO_2 + nNH_3 + sH_2 \quad \text{eq. (3)}$$

A biodegradability index (BI) was used to estimate the digestion efficiency via biochemical methane potential (BMP) assays. From eq. (3), the biodegradability index has been calculated as the ratio of the actual methane yield to the stoichiometric methane yield.

3. Results and discussion:

3.1 Coating effect of TiO_2 deposition onto zeolites using reactive magnetron sputtering

Being an effective deposition process, magnetron sputtering is typically considered to be a "line of sight" process, making it generally unsuitable to coat particulates. In contrast to that, addition of the oscillation mechanism has been shown to be effective in coating the particulated substrate, ranging from several nm to mm in size [18, 19, 23]. SEM images of the coated and uncoated zeolites are provided in Figure 3; it is obvious that deposition of titania coating did not exhibit a significant effect on the substrate morphology. Indeed, the coatings deposited with the oscillating substrate manipulation mechanism are typically reported to be uniformly distributed and generally replicating the morphology of the underlying substrate [23-24].

XRD analysis and EDX mapping of titanium was performed to ascertain the elemental composition of materials and distribution of Ti on the surface of the zeolite. The analysis was performed at five points; the mean values are presented in the Table 1, where a notable increase in titanium content from a negligible amount to 1.28 wt% can be observed. The XRD patterns of the uncoated and TiO_2 coated zeolite in Figure 4 evidence increased peaks at 22.5˚ and 36˚, which are attributed to the anatase crystal structure of TiO_2. This, alongside the EDX results, suggests that TiO_2 was successfully loaded onto the surface of the zeolite structure.

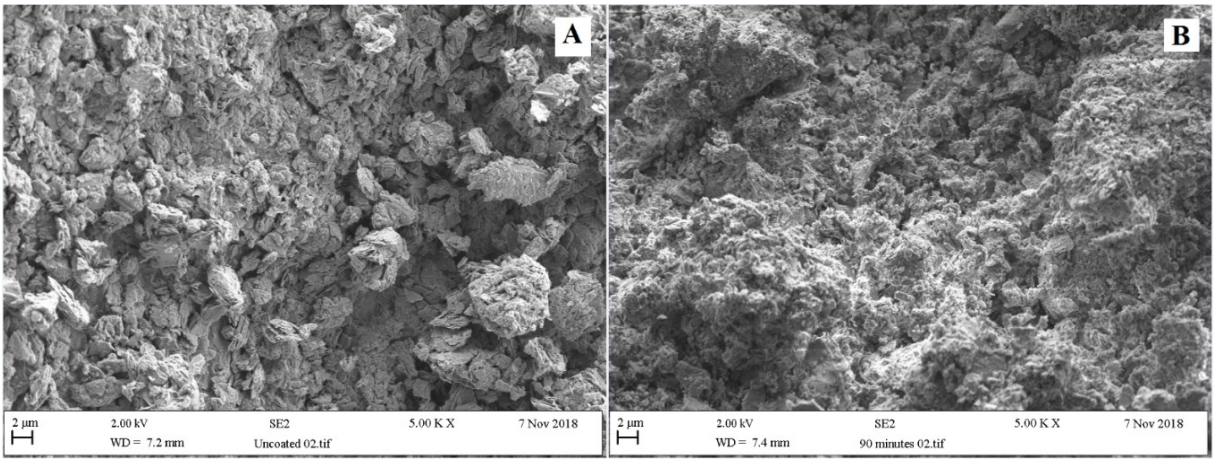

Figure 3 SEM images of uncoated (A) versus TiO_2 coated (B) zeolite surfaces

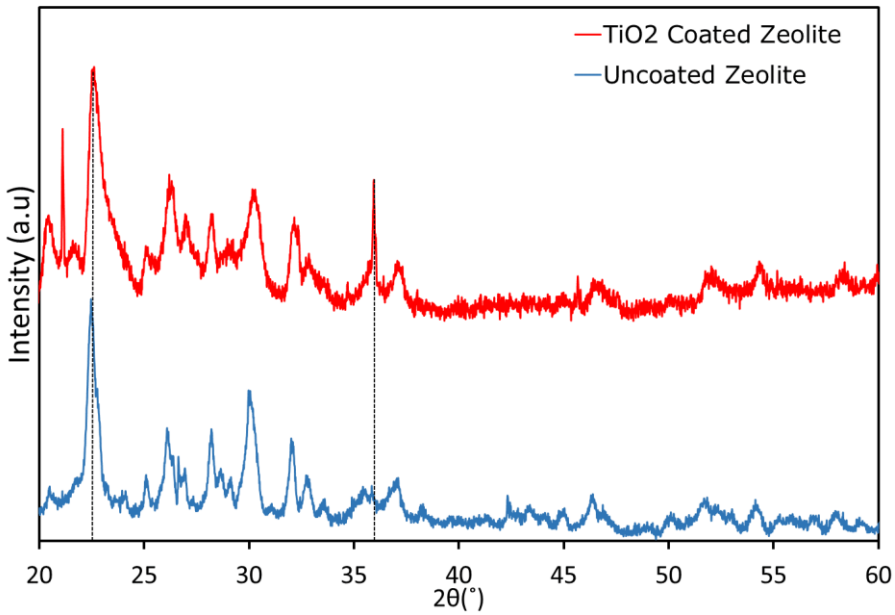

Figure 4 XRD patterns of the uncoated and TiO_2 coated zeolite

Table 1 Quantitative zeolite surface characterisation

Element	**Uncoated**		***Coated***	
	Wt%	**At%**	**Wt%**	**At%**
O	42.73	56.78	36.39	44.9
Na	0.14	0.13	0.22	0.19
Mg	1.01	0.89	0.59	0.48
Al	9.89	7.79	6.87	5.03
Si	35.96	27.22	32.03	22.51
K	1.52	0.83	2.34	1.18
Ca	2.9	1.54	3.68	1.81
Ti	-	-	1.28	0.53
Fe	3.97	1.51	3.05	1.08

Figure 5(a) shows adsorption-desorption isotherms of the uncoated and coated zeolite. Textural characteristics of the two samples are provided in Table 2. The isotherms were type II-b, characterised with a type H3 hysteresis and no plateau at high relative pressures. Such isotherms are usually obtained with aggregated particles containing slit-shaped pores and have been reported for clinoptilolite [25]. The surface area of the uncoated sample is low due to pore blocking by cations and presence of impurities [26]. Coating with TiO_2 did not affect the textural characteristics of the zeolite sample. The coating resulted in a slight increase in the BET surface area and total pore volume, which could be associated with the TiO_2 coating. The TiO_2 coating further reduced the accessibility of the micropores, which was evident from the increase in the external surface area and the decrease of the micropore area. The BJH pore size distributions, in Figure 5(b), indicate a slight increase in the broad pore 10-30 nm peak of the coated sample. Therefore, Figure 5 further confirms that the coating did not substantially influence the textural characteristics of the zeolite sample.

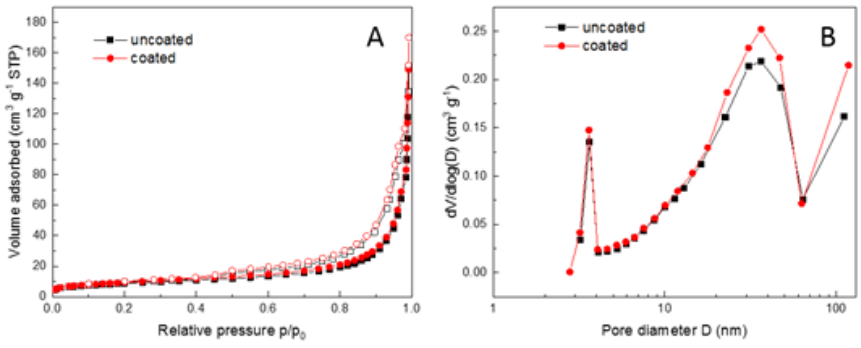

Figure 5 A - nitrogen adsorption desorption isotherms at -196 °C of uncoated and coated zeolite samples (solid symbols - adsorption; open symbols – desorption); B - Barrett-Joyner-Halenda (BJH) desorption pore-size distributions of uncoated and coated zeolite samples

Table 2 BET surface areas (S_{BET}), total pore volumes (V_{TOTAL}), external surface areas (S_{EXT}) and micropore areas (S_{MICRO}) of the uncoated and coated zeolite samples.

Sample	S_{BET} [$m^2\ g^{-1}$]	V_{TOTAL} [$cm^3\ g^{-1}$]	S_{EXT} [$m^2\ g^{-1}$]	S_{MICRO} [$m^2\ g^{-1}$]
Uncoated	31.2±0.20	0.21	28.0	3.3
TiO_2 Coated	33.7±0.16	0.23	32.0	1.8

3.2 Effect of photocatalytic pre-treatment on plant's morphology and methane yields

The initial cellulose, hemi-cellulose and (klason) lignin content in the *Miscanthus* biomass were identified at 38.27%, 24.67% and 17.95% respectively, based on total dry matter weight. SEM images of *Miscanthus* biomass in Figure 6 (a, b) indicate that UV treatment is effective at breaking down the plant's structure and the addition of TiO_2 supported zeolites as photocatalyst further contributes to open up the structure, increasing the surface area available to enzymes degradation. The photocatalysts appear to be lodging onto the biomass surface, maximising the action of UV irradiation locally to liberate available sugars. Analysis of the water soluble sugars (Table 3) show that there was an increase of glucose, fructose, xylose and galactose (22%, 13%, 82% and 17% respectively) when compared with the non-irradiated control. The significant increase in xylose indicates significant hemi-cellulose degradation and possibly exposure of the underlying cellulose structures, which is suggested by the increase in glucose. The XRD patterns of the untreated and UV treated miscanthus in Figure 6(c) show a decrease in the I_{002} diffraction peak at 22.5˚, which is associated with crystalline cellulose, with CI index reduction from 49.5% to 45.2%. The decrease in crystalline structures and increase in water soluble C6 sugars strongly suggests UV cellulose degradation.

Furthermore, as FTIR spectroscopy can characterise structural changes in the lignocellulose, Figure 6(c) shows the absorption spectra of the treated and untreated samples. Cellulose, hemicellulose and lignin share many similar absorption peaks such as 3346, 2860, 1029 cm^{-1} ascribed to O-H, C-H and C-O bonds respectively. However, the peak at 1372 (primarily attributed to cellulose) strongly decreases after UV treatment, confirming the positive treatment effect at reducing cellulose crystallinity. Additionally, a small decrease of the C=O peak at 1729 cm^{-1} associated with hemicellulose, suggests the measured increment of soluble xylose (Table 3) would be from structural hemicellulose. Lignin degradation evidenced by the decrease in peak intensities at 1648 and 833 cm^{-1}, attributed to C=O and C-H aromatic bonding respectively. An interesting work by Tsapekos et al. [27] reports production of phenolic

compounds from TiO_2–AgCl photocatalysis of lignin in wheat straw, which are toxic to anaerobic consortia. In this study, the concentration of phenolic and other aromatic structures was not measured after treatment however, BMP results discussed later in this section demonstrate no inhibition took place, meaning inhibitory levels were not reached during fermentation.

The partial UV degradation of the polysaccharide structures would not only increase the available surface area for microbial growth, but also reduce the recalcitrance of the remaining solids to enzymatic degradation [28].

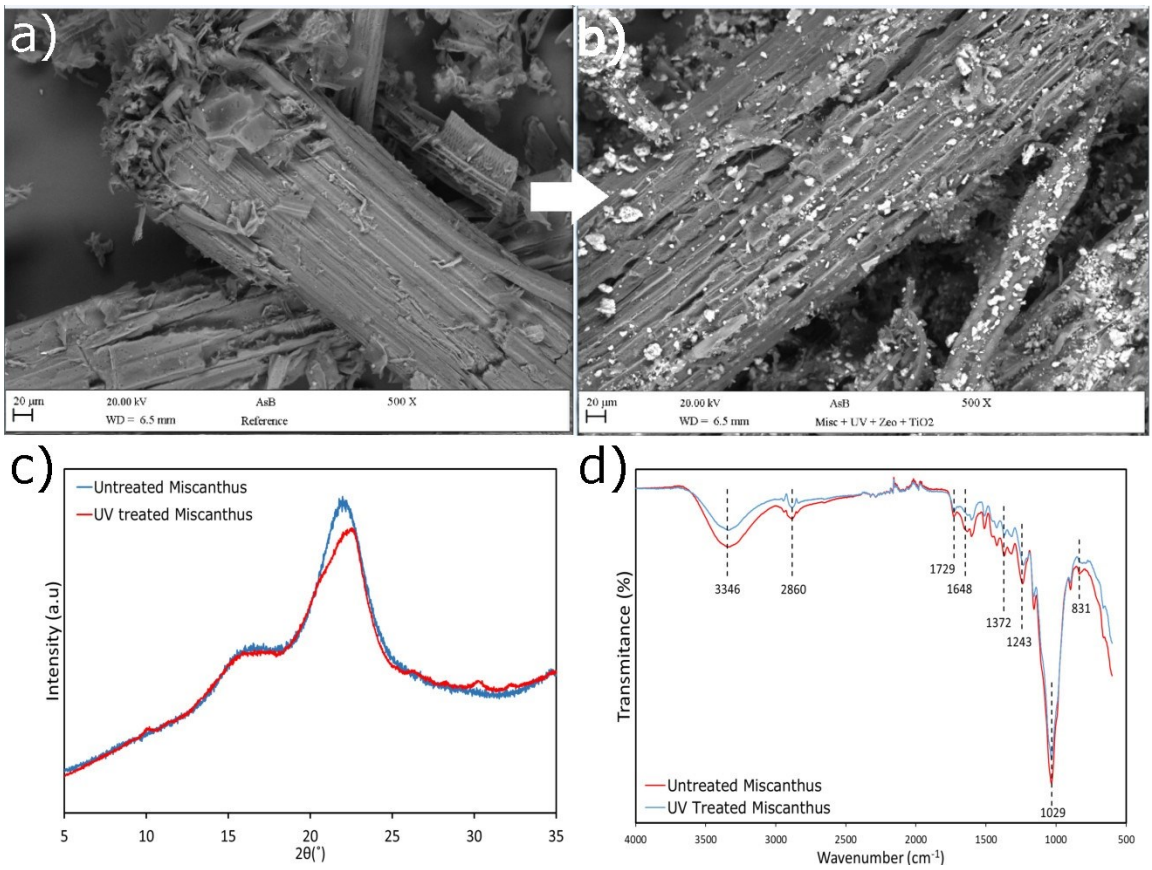

Figure 6 (a,b) SEM image of (a) untreated and (b) UV treated-3hours with 2.0% (w/w) TiO2 supported zeolites of Miscanthus biomass, (c) XRD and (d) FTIR spectra of miscanthus before and after treatment

Table 3 – Water soluble sugars after pre-treatment

Sugar	Untreated Control [mM]	UV Treated + TiO_2 supported zeolites [mM]	Change [%]
Glucose	1.36	1.66	+22.1%
Fructose	0.89	1.01	+13.0%
Xylose	0.54	0.99	+82.4%
Galactose	0.83	0.98	+17.3%

Results from the proximate and elemental analysis are described in Table 4. The VS% of the substrate is extremely high, with an Organic Matter Content (OMC) above 98%. This would normally lead to high potential for methane production. TS and VS contents are in line with values reported in the literature [29], with overall Ash-to-Volatile (A:V) ratios of 0.02 and 0.04 for *Miscanthus* and inoculated sludge respectively. These values anticipate healthy digester conditions. In fact, where digestion of substrates is characterised by high A:V indicators, this substantially results in decreased methane yield [30, 31]. From the ultimate analysis, it can be noticed that the C:N of the feedstock is out of range of the optimal digestion values (20-30) identified by Chen et al. [32] however, the inoculum-to-substrate ratio used in the BMP trials (4:1 w/w as per standard procedure) contributed to normalise this parameter much closer to the ideal range.

The stoichiometric (theoretical) methane yield (SMP) has been derived from the elemental characterisation in Table 4 and is reported in Table 5, along with the results of the BMP tests for all samples. Figure 7 shows instead the methane yields obtained from each sample in relation to the gaseous ammonia concentrations (ppm) detected by the GEOTech analyser.

Table 4 Feedstock and inoculum characterisation.

Feedstock	Proximate analysis					Ultimate analysis					
	TS %	VS %	OMC % (of TS)	Ash % (of TS)	A:V	C%	H%	N%	S%	O%	C:N
Miscanthus x giganteous	98.8 (0.01)	97.0 (0.01)	98.18	1.82 (0.01)	0.02	48.67 (0.03)	6.03 (0.04)	0.33 (0.01)	0.13 (0.03)	43.03 (0.01)	148
Inoculum	8.12 (0.02)	5.4 (0.15)	66.88	2.69 (0.15)	0.04	37.18 (0.98)	-	7.06 (0.16)	-	-	5

Abbreviations: TS=Total Solids; VS=Volatile Solids; OMC=Organic Matter Content; A:V=Ash-to-Volatile ratio

Table 5 Results of BMP trials at different conditions

Sample ID for AD	***Miscanthus x giganteous*** **[g]**	**Deionised water solution [mL]**	**Uncoated additive [% w./w.]**	**TiO_2-coated additive [% w./w.]**	**Photocatalytic treatment [hours]**	**SMP [mL_N gVS^{-1}]**	**CH_4% Theoretical**	**BMP [mL_N gVS^{-1}]**	**CH_4% Actual**	**BI [%]**	**H_2S [ppm]**
Inoculum	-	-	-	-	-	-	-	52.1±7	48	-	>1000
Inoculum + zeolites	-	50	2%	-	-	-	-	67.3±40	56	-	600
Untreated/control	2.5	50	-	-	-	477.2	51.6	118.2±50	48	0.25	>1000
UV-treated	2.5	50	-	2%	3			219.5±28	55	0.46	>1000

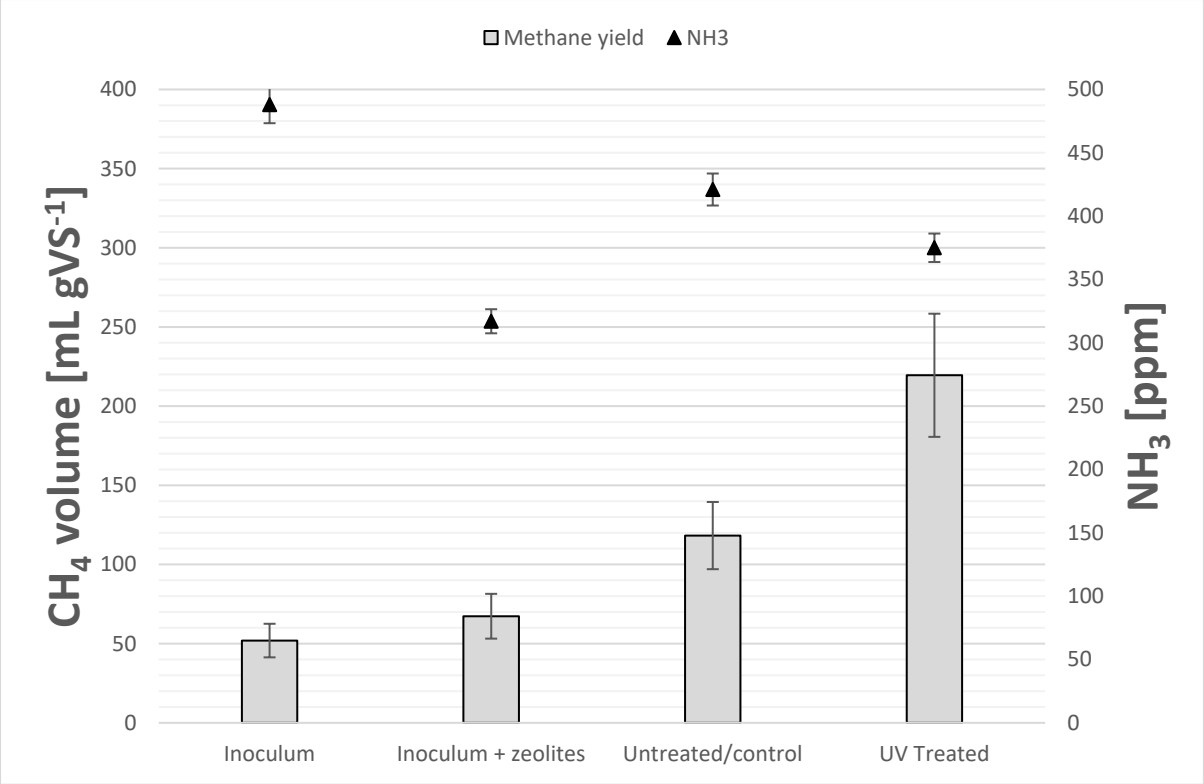

Figure 7 Methane yield in relation to ammonia content

The inoculum sludge produced about 850 mL and 1100 mL of methane across the digestion period with and without addition of zeolites respectively. This shows an improvement of about +10% in biogas volume and +23% extra methane yield, when inorganic additive is introduced. Despite the small amount (~20 g L^{-1}), the additive demonstrates great potential as AD enhancer increasing overall yields by reducing the ammonia content by 35% (from >488 to 317 ppm). Thanks to its cation exchange properties, clinoptilolite has high affinity for $NH4^{+}$ binding with the result of reducing the lag phase in AD. The kinetics of ammonia reduction by natural zeolite clinoptilolite structures [33] and their beneficial effects in AD systems have been investigated in detail elsewhere [34]. Readings of gaseous hydrogen sulfide were only possible below the threshold of the biogas analyser for the inoculum sludge with added zeolites (600ppm). The ability to absorb H_2S by zeolites is also reported by Casoli et al. [35] however, the fermentation of the substrate to methane clearly needs to be balanced by a larger additive amount to quantitatively appraise its contribution at reducing concentrations of this toxic compound. The positive effect of nano-structured materials on biogas has also been reported to be dosage dependant, according to a very recent work by Baniamerian et al. [36]. Some studies have also reported negative effects in methane production associated with high levels of natural inorganic adsorbents [37]. It appears this is due to excessive ion leaching that impairs bacterial balance,

with maximum beneficial thresholds identified between 5%-10% v./v., depending on additive composition.

The untreated substrate yielded 118.2 $mL_N\ gVS^{-1}$**,** which is in line with the values reported by Menardo et al. [29] and Tetteh et al [38]. A reduction in ammonia content of about 11% is observed between the treated and untreated sample, again showing effectiveness of the zeolite additive. The photolysed suspension exhibits a methane potential of about 220 $mL_N\ gVS^{-1}$, with an improvement of 13.5% and a significant 46.1% in biogas and methane yields respectively. Despite a remarkable increase in biodegradability index (from 0.25 to 0.46) from Table 5, there is still a wide margin for improvement with respect to the stoichiometric yields (SMP of 477 $mL_N\ gVS^{-1}$). Avoiding the use of harsh chemicals (acid or alkaline) is an obvious advantage of photocatalysis of lignocellulosics, which does not pose the inconvenient drawback of disposal or downstream processing for solvent recycling [39]. Most physical and mechanical treatments yield a methane increase (up to 30%-40%) [40-43], similar to those found in this study, although these results are found to be higher energy demanding than UV irradiation.

The enhancement of renewable gas yields found is only partially justified by the photocatalytic pretreatment, which served the purpose of depolymerising the lignin in the substrate into more useful AD metabolites (i.e. carboxylic acids, as reported by Colmenares et al. [8]). Another reason behind the improved yields is the composition of the zeolite additive. As reported in Table 1, the zeolites are constituted by different weighted %s of Na, Mg, Al, Si, K, Ca, Ti and Fe. Chen et al. [29] reviewed the major factors related to inhibition of the anaerobic digestion process. The authors report that light metal ions at low concentrations (Na, K, Mg, Ca, and Al) are required micronutrients for microbial growth, which is consequently stimulated by their presence. They also report that potassium enhances the AD performance in both the thermophilic and mesophilic regimes at concentrations less than 400 mg/L. Additionally, Demirel and Scherer [44] establish trace elements are required for biological conversion of agricultural substrates to methane, which include Fe in particular for growth of a range of methanogens. Finally, Garcia et al. [45] investigated in depth the effect of TiO_2, among others, at a concentration of 1.12 mg L^{-1} on the activity of microbial communities and found this is not toxic. The weight of all trace elements detected by the EDX analysis is lower than inhibitory values recorded in the literature and, therefore, we estimate they acted as methane boosters in the AD trials conducted.

3.3 Energy balance

An energy balance analysis was performed according to Alvado-Morales et al. [9], as described by eq. (4), considering the energy efficiency (η_p) of the UV treatment as function of the amount of substrate to be treated. In addition, a modified energy efficiency (η_U) equation that utilises as benchmark the energy output from the untreated substrate has been used to establish the economic viability of pretreating the substrate with respect to yields achievable when no treatment is applied (untreated). The latter is described by eq. (5).

$$\eta_p = 1 - E_{Pretreatment}/E_{CH4} \qquad \text{eq. (4)}$$

$$\eta_U = \eta_p - E_{Untreated}/E_{CH4} \qquad \text{eq. (5)}$$

In the simplified equations above, E_{CH4} is the heating value of the methane produced by the sample (10.27 kWh/m^3), while $E_{Pretreatment}$ is the energy consumption of the UV-lamp (200-400 nm) as calculated by Alvado-Morales et al. (0.061 kWh/min for each m^3 of suspension treated) and is considered as the only energy expenditure in the calculations of energy efficiencies.

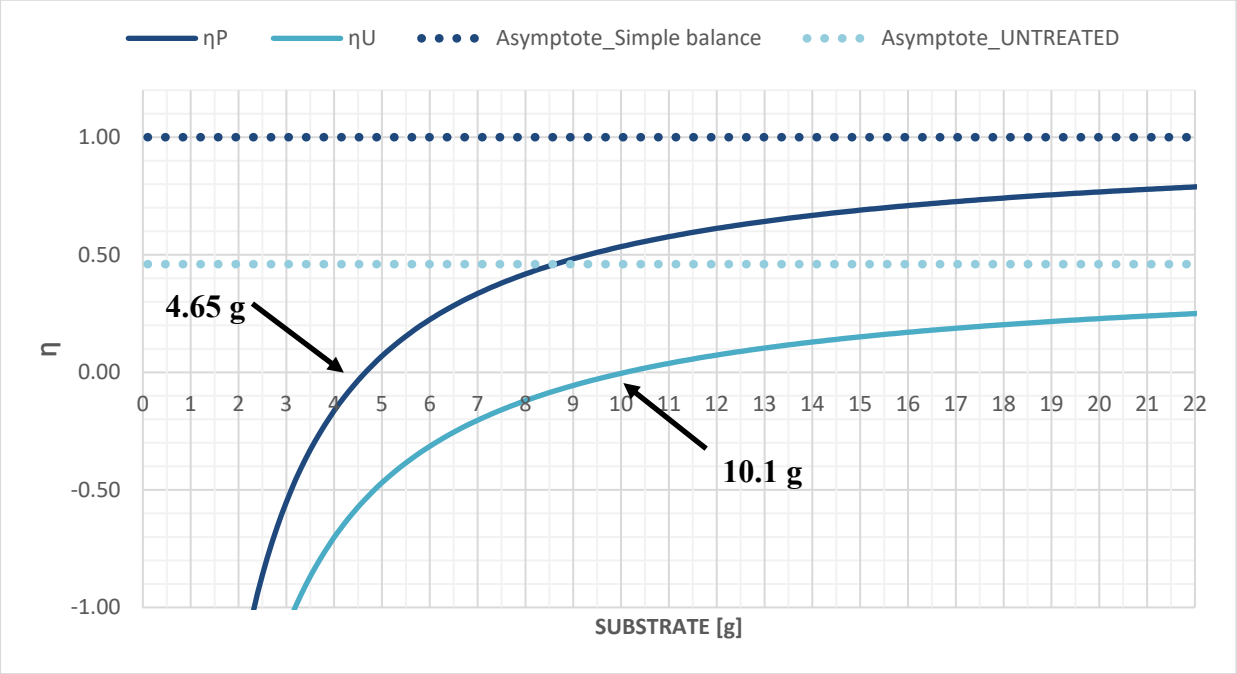

Figure 8 Energy efficiencies of the photocatalytic pretreatment

Results of the energy balance analysis are plotted in Figure 8, where $E_{Pretreatment} = 0$ represent each asymptotic limit for the functions described by eq. (4) and (5). As it can be observed, the

photocatalytic treatment pays off at a break-even point of 4.65 g of substrate treated in 1 m^3 of suspension and the net energy balance is positive for greater values. However, it is only above a suspended concentration of 10.1 g m^{-3} that the pretreatment becomes economically convenient as the resulting net energy balance is greater than the untreated (E_{CH4} - $E_{Pretreatment}$ > $E_{Untreated}$).

This overall confirms the findings of Uellendahl et al. [46], which also reported an increased ratio of energy output to input costs when fermenting perennial crops by wet pre-treated oxidation. This essentially makes perennial crops and particularly Miscanthus crops, as identified by these results, competitive to the use of maize for biomethane production.

4. Conclusion:

This study was able to establish that photocatalytic pretreatment of perennial crops can enhance rates of biogas volume and quality (dictated by the methane content) achievable from the feedstock. The biodegradability index of the substrate improved over 45% through the treatment with TiO_2 coated zeolites. However, being the biodegradability of the treated sample 0.46, there is a clear indication that more studies are needed to get nearer stoichiometric values of biomethane potential. These should focus on customised (biomass type dependent) variations of annealing time of the photocatalyst coat onto the zeolite supports and different concentrations of catalyst load in the reactor, along with varying UV treatment duration.

A boost in methane yield was achieved (up to 220 mL_N gVS^{-1}) by the photolysed sample of *Miscanthus x giganteous* biomass, which also contained traces of important microbial nutrients such as Na, Mg, Al, Si, K, Ca, and Fe as part of the structure of the microporous zeolite used to support the TiO_2 coatings. It can be concluded that the zeolite supports and the photocatalytic pretreatment had a synergistic effect in contributing to higher methane yields from the substrate. The net energy balance carried out identified the treatment is economically convenient with respect to the untreated *Miscanthus* for substrate concentrations above 10.1 g m^{-3} in the suspended solution.

Acknowledgements

This research was supported by Manchester Metropolitan University via the Research Accelerator Award (RAG 2017/18 - 113380) and the Advanced Materials and Surface Engineering (AMSE) Research Centre's Incentivisation award. BBSRC NIBB's network High Value from Plants (Phase I) funded the training and compositional analysis of biomass in conjunction with Celignis ltd. (CORE-TA – 19).

References

[1] Zeng, Y., Zhao, S., Yang, S. and Ding, S.Y., 2014. Lignin plays a negative role in the biochemical process for producing lignocellulosic biofuels. *Current opinion in biotechnology*, *27*, pp.38-45.

[2] Monlau, F., Sambusiti, C., Barakat, A., Guo, X.M., Latrille, E., Trably, E., Steyer, J.P. and Carrere, H., 2012. Predictive models of biohydrogen and biomethane production based on the compositional and structural features of lignocellulosic materials. *Environmental science & technology*, *46*(21), pp.12217-12225.

[3] Liu, X., Bayard, R., Benbelkacem, H., Buffière, P. and Gourdon, R., 2015. Evaluation of the correlations between biodegradability of lignocellulosic feedstocks in anaerobic digestion process and their biochemical characteristics. *Biomass and Bioenergy*, *81*, pp.534-543.

[4] Brosse, N., Dufour, A., Meng, X., Sun, Q. and Ragauskas, A., 2012. Miscanthus: a fast-growing crop for biofuels and chemicals production. *Biofuels, Bioproducts and Biorefining*, *6*(5), pp.580-598.

[5] Yoshida, M., Liu, Y., Uchida, S., Kawarada, K., Ukagami, Y., Ichinose, H., Kaneko, S. and Fukuda, K., 2008. Effects of cellulose crystallinity, hemicellulose, and lignin on the enzymatic hydrolysis of Miscanthus sinensis to monosaccharides. *Bioscience, biotechnology, and biochemistry*, *72*(3), pp.805-810.

[6] Kiesel, A. and Lewandowski, I., 2017. Miscanthus as biogas substrate–Cutting tolerance and potential for anaerobic digestion. *Gcb Bioenergy*, *9*(1), pp.153-167.

[7] Li, S.H., Liu, S., Colmenares, J.C. and Xu, Y.J., 2016. A sustainable approach for lignin valorization by heterogeneous photocatalysis. *Green Chemistry*, *18*(3), pp.594-607.

[8] Colmenares, J.C. and Luque, R., 2014. Heterogeneous photocatalytic nanomaterials: prospects and challenges in selective transformations of biomass-derived compounds. *Chemical Society Reviews*, *43*(3), pp.765-778.

[9] Alvarado-Morales, M., Tsapekos, P., Awais, M., Gulfraz, M. and Angelidaki, I., 2017. TiO2/UV based photocatalytic pretreatment of wheat straw for biogas production. *Anaerobe*, *46*, pp.155-161.

[10] Serrano, D.P., Aguado, J., Rodriguez, J.M. and Peral, A., 2008. Effect of the organic moiety nature on the synthesis of hierarchical ZSM-5 from silanized protozeolitic units. *Journal of materials chemistry*, *18*(35), pp.4210-4218.

[11] Weiß, S., Zankel, A., Lebuhn, M., Petrak, S., Somitsch, W. and Guebitz, G.M., 2011. Investigation of mircroorganisms colonising activated zeolites during anaerobic biogas production from grass silage. *Bioresource technology*, *102*(6), pp.4353-4359.

[12] Sluiter, A., Hames, B., Ruiz, R., Scarlata, C., Sluiter, J. and Templeton, D., 2008. Determination of ash in biomass. Laboratory Analytical Procedure (LAP). National Renewable Energy Laboratory.

[13] Standard, C.E.N. and EN, B., 2011. 15104: 2011 Solid biofuels–Determination of total content of carbon, hydrogen and nitrogen–instrumental methods, in.

[14] Sluiter, A., Hames, B., Hyman, D., Payne, C., Ruiz, R., Scarlata, C., Sluiter, J., Templeton, D. and Wolfe, J., 2008. Determination of total solids in biomass and total dissolved solids in liquid process samples. *National Renewable Energy Laboratory, Golden, CO, NREL Technical Report No. NREL/TP-510-42621*, pp.1-6.

[15] Sluiter, A., Hames, B., Ruiz, R., Scarlata, C., Sluiter, J., Templeton, D. and Crocker, D., 2008. Determination of structural carbohydrates and lignin in biomass. *Laboratory analytical procedure*, *1617*, pp.1-16.

[16] Segal, L., Creely, J.J., Martin Jr., A.E., Conrad, C.M., 1959. An empirical method for estimating the degree of crystallinity of native cellulose using the X-ray diffractometer. Text. Res. J. 29, 786–794.

[17] Ratova, M., Kelly, P., West, G. and Tosheva, L., 2016. A novel technique for the deposition of bismuth tungstate onto titania nanoparticulates for enhancing the visible light photocatalytic activity. *Coatings*, *6*(3), p.29.

[18] Ratova, M., Kelly, P.J., West, G.T., Tosheva, L. and Edge, M., 2017. Reactive magnetron sputtering deposition of bismuth tungstate onto titania nanoparticles for enhancing visible light photocatalytic activity. *Applied Surface Science*, *392*, pp.590-597.

[19] Ratova, M., Kelly, P.J., West, G.T. and Iordanova, I., 2013. Enhanced properties of magnetron sputtered photocatalytic coatings via transition metal doping. *Surface and Coatings Technology*, *228*, pp.S544-S549.

[20] Ortiz-Gomez, A., Serrano-Rosales, B., Salaices, M. and de Lasa, H., 2007. Photocatalytic oxidation of phenol: reaction network, kinetic modeling, and parameter estimation. *Industrial & Engineering Chemistry Research*, *46*(23), pp.7394-7409.

[21] Verein Deutscher Ingenieure, VDI 4630, Düsseldorf. Fermentation of organic materials. Characterisation of substrate, sampling, collection of material data, fermentation tests [1872] VDI Gesellschaft Energietechnik; 2006.

[22] Buswell, A.M. and Boruff, C.S., 1932. The relation between the chemical composition of organic matter and the quality and quantity of gas produced during sludge digestion. *Sewage Works Journal*, pp.454-460.

[23] Ratova, M., Marcelino, R., de Souza, P., Amorim, C. and Kelly, P., 2017. Reactive Magnetron Sputter Deposition of Bismuth Tungstate Coatings for Water Treatment Applications under Natural Sunlight. *Catalysts*, *7*(10), p.283.

[24] Ratova, M., Redfern, J., Verran, J. and Kelly, P.J., 2018. Highly efficient photocatalytic bismuth oxide coatings and their antimicrobial properties under visible light irradiation. *Applied Catalysis B: Environmental*, *239*, pp.223-232.

[25] Rouquerol, J., Rouquerol, F., Llewellyn, P., Maurin, G. and Sing, K.S., 2013. *Adsorption by powders and porous solids: principles, methodology and applications*. Academic press.

[26] Korkuna, O., Leboda, R., Skubiszewska-Zie, B.J., Vrublevs'Ka, T., Gun'Ko, V.M. and Ryczkowski, J., 2006. Structural and physicochemical properties of natural zeolites: clinoptilolite and mordenite. *Microporous and Mesoporous Materials*, *87*(3), pp.243-254.

[27] Tsapekos, P., Alvarado-Morales, M., Boscaro, D., Mazarji, M., Sartori, L. and Angelidaki, I., 2018. TiO2–AgCl based nanoparticles for photocatalytic production of phenolic compounds from lignocellulosic residues. *Energy & fuels*, *32*(6), pp.6813-6822.

[28] Murnen, H.K., Balan, V., Chundawat, S.P., Bals, B., Sousa, L.D.C. and Dale, B.E., 2007. Optimization of ammonia fiber expansion (AFEX) pretreatment and enzymatic hydrolysis of Miscanthus x giganteus to fermentable sugars. *Biotechnology progress*, *23*(4), pp.846-850.

[29] Menardo, S., Bauer, A., Theuretzbacher, F., Piringer, G., Nilsen, P.J., Balsari, P., Pavliska, O. and Amon, T., 2013. Biogas production from steam-exploded Miscanthus and utilization of biogas energy and CO 2 in greenhouses. *BioEnergy Research*, *6*(2), pp.620-630.

[30] Tedesco, S. and Daniels, S., 2018. Optimisation of biogas generation from brown seaweed residues: Compositional and geographical parameters affecting the viability of a biorefinery concept. *Applied Energy*, *228*, pp.712-723.

[31] Tedesco, S. and Daniels, S., 2019. Evaluation of inoculum acclimatation and biochemical seasonal variation for the production of renewable gaseous fuel from biorefined Laminaria sp. waste streams. *Renewable energy*, *139*, pp.1-8.

[32] Chen, Y., Cheng, J.J. and Creamer, K.S., 2008. Inhibition of anaerobic digestion process: a review. *Bioresource technology*, *99*(10), pp.4044-4064.

[33] Kithome, M., Paul, J.W., Lavkulich, L.M. and Bomke, A.A., 1998. Kinetics of ammonium adsorption and desorption by the natural zeolite clinoptilolite. *Soil Science Society of America Journal, 62(3),* pp.622-629.

[34] Wang, X., Zhang, L., Xi, B., Sun, W., Xia, X., Zhu, C., He, X., Li, M., Yang, T., Wang, P. and Zhang, Z., 2015. Biogas production improvement and C/N control by natural clinoptilolite addition into anaerobic co-digestion of Phragmites australis, feces and kitchen waste. *Bioresource technology, 180,* pp.192-199.

[35] Cosoli, P., Ferrone, M., Pricl, S. and Fermeglia, M., 2008. Hydrogen sulphide removal from biogas by zeolite adsorption: Part I. GCMC molecular simulations. *Chemical Engineering Journal*, *145*(1), pp.86-92.

[36] Baniamerian, H., Isfahani, P.G., Tsapekos, P., Alvarado-Morales, M., Shahrokhi, M., Vossoughi, M. and Angelidaki, I., 2019. Application of nano-structured materials in anaerobic digestion: Current status and perspectives. *Chemosphere*.

[37] Tada, C., Yang, Y., Hanaoka, T., Sonoda, A., Ooi, K. and Sawayama, S., 2005. Effect of natural zeolite on methane production for anaerobic digestion of ammonium rich organic sludge. *Bioresource technology*, *96*(4), pp.459-464.

[38] Tetteh, E.K., Amano, K.A., Asante-Sackey, D. and Armah, E.K., 2017. Biochemical Methane Potential (BMP) of Miscanthus Fuscus for Anaerobic Digestion. *International Journal of Scientific and Research Publications*, *7*(12), pp.434-439.

[39] Den, W., Sharma, V.K., Lee, M., Nadadur, G. and Varma, R.S., 2018. Lignocellulosic biomass transformations via greener oxidative pretreatment processes: Access to energy and value-added chemicals. *Frontiers in chemistry*, *6*.

[40] Zheng, Y., Zhao, J., Xu, F. and Li, Y., 2014. Pretreatment of lignocellulosic biomass for enhanced biogas production. *Progress in energy and combustion science*, *42*, pp.35-53.

[41] Bruni, E., Jensen, A.P. and Angelidaki, I., 2010. Comparative study of mechanical, hydrothermal, chemical and enzymatic treatments of digested biofibers to improve biogas production. *Bioresource technology*, *101*(22), pp.8713-8717.

[42] Kobayashi, F., Take, H., Asada, C. and Nakamura, Y., 2004. Methane production from steam-exploded bamboo. *Journal of bioscience and bioengineering*, *97*(6), pp.426-428.

[43] Jackowiak, D., Frigon, J.C., Ribeiro, T., Pauss, A. and Guiot, S., 2011. Enhancing solubilisation and methane production kinetic of switchgrass by microwave pretreatment. *Bioresource technology*, *102*(3), pp.3535-3540.

44] Demirel, B. and Scherer, P., 2011. Trace element requirements of agricultural biogas digesters during biological conversion of renewable biomass to methane. *Biomass and bioenergy*, *35*(3), pp.992-998.

[45] García, A., Delgado, L., Torà, J.A., Casals, E., González, E., Puntes, V., Font, X., Carrera, J. and Sánchez, A., 2012. Effect of cerium dioxide, titanium dioxide, silver, and gold nanoparticles on the activity of microbial communities intended in wastewater treatment. *Journal of hazardous materials*, *199*, pp.64-72.

[46] Uellendahl, H., Wang, G., Møller, H.B., Jørgensen, U., Skiadas, I.V., Gavala, H.N. and Ahring, B.K., 2008. Energy balance and cost-benefit analysis of biogas production from perennial energy crops pretreated by wet oxidation. *Water science and technology*, *58*(9), pp.1841-1847.